A Method of Planar-Template-Based Camera Self-Calibration for Single-View

Yue Zhao and Chao Li

Abstract—Camera calibration is an important step in 3D reconstruction. Camera calibration may be classified into two major types: traditional calibration and self-calibration. However, a calibration method in using a checkerboard is intermediate between traditional calibration and self-calibration. A self-calibration algorithm is proposed based on a square in this paper. Only a square in the planar template, the camera self-calibration can be completed through the single view. The proposed algorithm is that the virtual circle and straight line are established by a square on planar template, and circular points, vanishing points in straight lines and the relationship between them are be used, in order to obtain the image of the absolute conic (IAC) and establish the camera intrinsic parameters. To make the calibration template is simpler, as compared with the Zhang Zhengyou's method. Through real experiments and simulation experiments, the experimental results show that this algorithm is feasible and available, and has a certain precision and robustness.

Keywords—Absolute conic, **c**amera calibration, circle point, vanishing point.

I. INTRODUCTION

IN the process of acquiring three-dimensional (3D) information from two-dimensional (2D) image, the camera calibration is an indispensable step. Camera calibration usually is divided into two classes: traditional calibration and self-calibration. The traditional calibration approach needs to prepare a high precision geometric calibration object, and then uses the relationship between world coordinate and image coordinate of calibration object to complete the camera calibration. In 1992, Hartley and Faugeras first put forward the thought of camera self-calibration, which was called camera self-calibration by using corresponding relationship of images. Now, camera self-calibration has become one of hot spot in computer vision [1-7]. Zhang Zhengyou (2000) [8] put forward one kind more flexible and simple calibration method which was to use a dot matrix template instead of traditional calibration object to solve linearly camera intrinsic parameters via homography between dot matrix and image. On the basis of Zhang Zhengyou's calibration method, Meng Xiaoqiao and Hu Zhanyi (2002) [9] put forward a kind of self-calibration method based on planar circle, which first introduced the concept of circular points into the technology of camera self-calibration. From then on, the technology of camera self-calibration enters a new field—the self-calibration by using circular points. Then,

many self-calibration methods appear in succession based on Zhang Zhengyou and Meng Xiaoqiao. Wu Fuchao et al. (2003) [10], a kind of camera self-calibration method was proposed by using two non-parallel rectangles in space plane to solve circular points. In addition, Li Xinju et al. (2004) [11] analyzed the shortage of Zhang Zhengyou's calibration method and put forward a kind of camera self-calibration method according to the similarity of plane scene image. Wang Guanghui (2008) [12] proposed a kind of camera self-calibration method using calibration object similar to Zhang Zhengyou's checkerboard based on Kruppa equation. In recent years, a large number of self-calibration methods based on circular points or vanishing points have emerged [13-16]. However, in this paper, we use a square as calibration object to solve camera intrinsic parameters by circular points, vanishing point and projective invariance.

II. CAMERA MODEL

In this paper, we use perspective projection model which corresponds to a pinhole camera model (Fig.1).
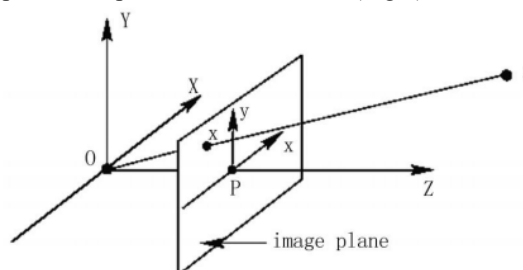

Fig. 1 Pinhole camera model

Let the world coordinate of a point (X) in space be $\begin{pmatrix} X & Y & Z \end{pmatrix}$ and the corresponding image coordinates be $\begin{pmatrix} u & v \end{pmatrix}$. $\begin{pmatrix} u_0 & v_0 \end{pmatrix}$ is the coordinates of principal point and s is skew factor. f_u, f_v represent the focal length of the lens. $\begin{pmatrix} r_{ij} \end{pmatrix}$ and $\begin{pmatrix} t_x & t_y & t_z \end{pmatrix}$ are rotation matrix and translation vector. So, the perspective projection matrix may be expressed

$$\lambda \begin{bmatrix} u \\ v \\ 1 \end{bmatrix} = K \begin{bmatrix} R & T \end{bmatrix} \begin{bmatrix} X \\ Y \\ Z \\ 1 \end{bmatrix}$$

Yue Zhao is with the School of Mathematics and Statistics, Yunnan University, Kunming, 650091 , China (phone: +86-871-5033700; fax: +86-871-5033700; e-mail: zhao6685@ yahoo.com.cn).
Chao Li is with the School of Mathematics and Statistics, Yunnan University, Kunming, 650091, China (e-mail: lc198746@126.com).

World Academy of Science, Engineering and Technology
International Journal of Mathematical and Computational Sciences
Vol:5, No:12, 2011

$$= \begin{bmatrix} f_u & s & u_0 \\ 0 & f_v & v_0 \\ 0 & 0 & 1 \end{bmatrix} \begin{bmatrix} r_{11} & r_{12} & r_{13} & t_1 \\ r_{21} & r_{22} & r_{23} & t_2 \\ r_{31} & r_{32} & r_{33} & t_3 \end{bmatrix} \begin{bmatrix} X \\ Y \\ Z \\ 1 \end{bmatrix}, \quad (1)$$

where K is camera intrinsic parameters in Equation (1). In this paper, the calibration object is a square on a planar template, so the planar template containing square may be defined as $X - Y$ plane of world coordinate system (WCS) and the coordinate Z of space points is always zero. Now, the simplified expressions of perspective projection model can be obtained

$$\lambda \begin{bmatrix} u \\ v \\ 1 \end{bmatrix} = H \begin{bmatrix} X \\ Y \\ Z \\ 1 \end{bmatrix} = \begin{bmatrix} f_u & s & u_0 \\ 0 & f_v & v_0 \\ 0 & 0 & 1 \end{bmatrix} \begin{bmatrix} r_{11} & r_{12} & t_1 \\ r_{21} & r_{22} & t_2 \\ r_{31} & r_{32} & t_3 \end{bmatrix} \begin{bmatrix} X \\ Y \\ Z \\ 1 \end{bmatrix}, \quad (2)$$

where H is called homography matrix from 3D to 2D coordinates.

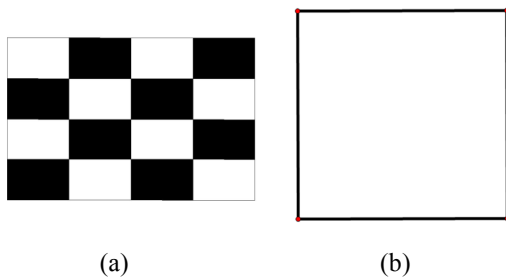## III. Camera Self-Calibration

(a)   (b)

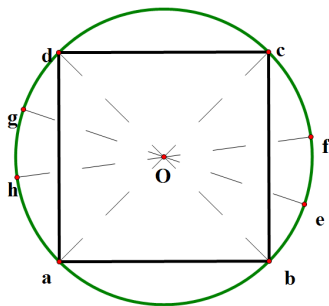Fig. 2 (a) and (b) are calibration template in literature [12] and this paper, respectively

Fig. 3 Virtual calibration template in this paper

Zhang Zhengyou [8] and Wang Guanghui's [12] self-calibration template is in Fig. 2 (a). The calibration template of this paper is in Fig. 2 (b). A virtual calibration template based on Fig. 2(a) is in Fig. 3. Without loss of generality, assume the planar template containing square (Fig. 2 (b)) is $X - Y$ plane of WCS, in which the origin is a, and X-axis, Y-axis are ab, ad, respectively. We can get the following conclusion. Several conclusions are drawn.

Lemma 1. If in Fig. 3, let the side length of square be a on the planar template, the equations of virtual circle and virtual lines can be determined, and the virtual lines cut the virtual circle at

e, f, g, h, lines ac, bd cut the virtual circle at a, b, c, d are known.

Proof. Suppose the center of the virtual circle is O where the two diagonals of a square *abcd* cross and a length of the diagonal is its diameter, as shown in Fig. 3, the coordinates of the center of a circle is $(a/2, a/2, 0)$ in the WCS, and the algebraic equation of the virtual circle in $X - Y$ plane is

$$\left(x - \frac{a}{2}\right)^2 + \left(y - \frac{a}{2}\right)^2 = 2a^2. \quad (3)$$

So the virtual lines are arbitrary lines through the center O of the virtual circle, without loss of generality, assuming that slopes of the virtual lines ge, hf are k_1, k_2, the equations of *ge*, *hf* are

$$\begin{aligned} y_1 &= k_1 x_1 + b_1, \\ y_2 &= k_2 x_2 + b_2 \end{aligned} \quad (4)$$

Take line *ge* as an example to seek the intersection of virtual circle and virtual line. As the virtual line passes through the center $O(a/2, a/2)$ of the virtual circle, replacing Equation (4), we can get

$$\frac{a}{2} = k_1 \frac{a}{2} + b_1,$$

arrange

$$b_1 = \frac{a}{2}(1 - k_1), \quad (5)$$

and finally determine line *ge*. Combining Equations (3), (4) and (5), we can get

$$\left(1 + k_1^2\right)x_1^2 + \left(2k_1 b_1 - ak_1 - a\right)x_1 + \left(\frac{a^2}{2} + b_1^2 - ab_1 - 2a^2\right) = 0. \quad (6)$$

Solve the monodic quadratic equation (Equation (6)) to get two intersections, and then the coordinates of the virtual lines and circle can be obtained through Equation (4).

Lemma 2. Assuming that homography matrix H from 3D to 2D coordinates is known, image coordinates of any 3D points of the planar template can be obtained in image coordinate system (ICS), particularly, circular points also can be gotten in ICS.

Proof. From Equation (2), Lemma 2 is obviously true. Particularly, $\begin{bmatrix} 1 & \pm i & 0 \end{bmatrix}^T$ are two circular points of the calibration plane in the WCS, so the image coordinates of circular points are unique

$$\begin{cases} m_i \approx H \begin{bmatrix} 1 & +i & 0 \end{bmatrix}^T \\ m_j \approx H \begin{bmatrix} 1 & -i & 0 \end{bmatrix}^T \end{cases}.$$

Obviously, homography matrix H can be estimated by at least four matching points. In Fig. 3, the image coordinates of four vertices a, b, c, d in the square can be obtained by Harris Corner Detection [17] and the world coordinates of a, b, c, d are obviously known, so H is estimated by four pairs of matching points. Combining Lemma 1 and Lemma 2, the image coordinates e, f, g, h, O and the circular points m_i, m_j can be gotten.

World Academy of Science, Engineering and Technology
International Journal of Mathematical and Computational Sciences
Vol:5, No:12, 2011

Lemma 3. Suppose v_1, v_2 are vanishing points on mutually orthogonal directions, $v_1^T \omega v_2 = 0$ ($\omega = K^{-T}K^{-1}$ is IAC).

Proof. Let $p_{1\infty}$, $p_{2\infty}$ be points at infinity on mutually orthogonal directions, of which image coordinates are v_1, v_2. According to the camera model with imaging principles, we have

$$\lambda_1 v_1 = K\begin{bmatrix} R & T \end{bmatrix} p_{1\infty}, \lambda_2 v_2 = K\begin{bmatrix} R & T \end{bmatrix} p_{2\infty}, \qquad (7)$$

and Equation (7) can be rewritten as

$$\begin{bmatrix} R & T \end{bmatrix} p_{1\infty} = \lambda_1 K^{-1} v_1, \begin{bmatrix} R & T \end{bmatrix} p_{2\infty} = \lambda_2 K^{-1} v_2.$$

From orthogonality in projective geometry, we have

$$\lambda_1 \lambda_2 v_1^T K^{-T} K^{-1} v_2 = p_{1\infty}^T \begin{bmatrix} R & T \end{bmatrix}^T \begin{bmatrix} R & T \end{bmatrix} p_{2\infty} = 0,$$

and therefore

$$v_1^T K^{-T} K^{-1} v_2 = 0.$$

In Fig. 3, $ab // cd$, the intersection of lines ab and cd is a point at infinity of which image is called vanishing point, denoted as v_1. Similarly, vanishing points of lines ad and bc, line ac and line bd are denotes as v_2, v_3 and v_4, respectively. Obviously, $v_1 \perp v_2, v_3 \perp v_4$, with Lemma 3, two constraint equations about IAC ω may be gotten

$$\begin{cases} v_2^T \omega v_1 = 0 \\ v_4^T \omega v_3 = 0 \end{cases}, \qquad (8)$$

where v_1, v_2 can be obtained by solving image intersections of lines ab, cd and lines bc, ad, respectively, and v_3, v_4 can also be obtain from following lemma.

Lemma 4. Supposing $P_i \in l(P)$ $(i = 1, 2, 3, 4)$ and $(P_1 P_2, P_3 P_4) = k\, (k \neq 0, 1, \infty)$, where three of P_1, P_2, P_3, P_4 and k are known, the fourth point can be determined. ($l(P)$ is point-set of line l .)

Proof. Supposing that homogeneous coordinates of P_1, P_2, P_3, P_4 are $a, b, a + \lambda_1 b, a + \lambda_2 b$, have

$$(P_1 P_2, P_3 P_4) = \frac{\lambda_1}{\lambda_2} = k. \qquad (9)$$

Without loss of generality, assuming that known P_1, P_2, P_3 are $a, b, a + \lambda_1 b$, now the solution of the fourth point is transformed to determine λ_2. From Equation (9), we have

$$\lambda_2 = \frac{\lambda_1}{k}. \qquad (10)$$

Supposing that homogeneous coordinates of P_1, P_2, P_3 are equal to $(u_1 \quad v_1 \quad 1)$, $(u_2 \quad v_2 \quad 1)$, $(u_3 \quad v_3 \quad 1)$, combining with $P_3 = a + \lambda_1 b$, we have

$$u_3 = \frac{u_1 + \lambda_1 u_2}{1 + \lambda_1}. \qquad (11)$$

Equation (11) can be rewritten as:

$$\lambda_1 = \frac{u_1 - u_3}{u_3 - u_2}. \qquad (12)$$

Combining with Equation (10) and (12), λ_2 can be obtained, and then P_4 can be determined.

As shown in Fig. 3, take line ac as an example to discuss how to solve a vanishing point of diameter of the virtual circle. In *Lemma 4.* If let $P_1 = a, P_2 = o, P_3 = c$, $P_4 = P_\infty$, it is reasonable assumption that the length of $P_1 P_\infty$ and $P_3 P_\infty$ are equal, and $\frac{P_1 P \infty}{P_3 P \infty} = 1$. Based on perspective projection, have $(P_1 P_3, P_2 P_\infty) = \frac{P_1 P_2}{P_3 P_2} = (P_1 P_3 P_2)$, where $P_1 P_3$ is the diameter and P_2 is the centre of the virtual circle, respectively, and $(P_1 P_3, P_2 P_\infty) = -1$. Additionally, under the projective transformation group, some graphics have projective properties and projective invariants. Combining with Lemma 4, we have

$$\begin{cases} (P_1 P_3, P_2 P_\infty) = -1 \\ P_1 P_3 \times P_1 P_\infty = 0 \end{cases}. \qquad (13)$$

Supposing the image coordinate of P_∞ is $(u_\infty, v_\infty, 1)$, the matrix expression of Equation (13) is

$$\begin{pmatrix} 1 & 0 \\ 0 & 1 \\ v_1 - v_2 & u_2 - u_1 \end{pmatrix} \begin{pmatrix} u_\infty \\ v_\infty \end{pmatrix} = \begin{pmatrix} u_\infty(u_2 + u_1) - 2u_1 u_2 / 2u_\infty - u_1 - u_2 \\ v_\infty(v_2 + v_1) - 2v_1 v_2 / 2v_\infty - v_1 - v_2 \\ u_2 v_1 - u_1 v_2 \end{pmatrix}. \qquad (14)$$

The image coordinate of P_∞ can be obtained by the method of least squares to solve Equation (14). Similarly, points at infinity of any diameter of the virtual circle are gotten.

Lemma 5 [19, 20]. The sufficient and necessary conditions of which two non-isotropic lines are mutually orthogonal are that points at infinity of the two non-isotropic lines are conjugated with two circular points of the plane where the two non-isotropic lines are.
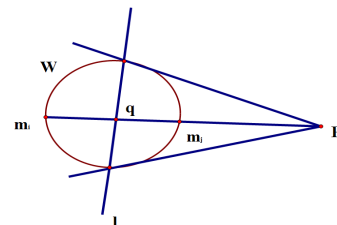

Fig. 4 An image of a plane at infinity

Fig. 4 is an image of a plane at infinity, where ω is absolute conic, m_i, m_j are two circular points of the plane π with the line at infinity pq. P is the point at infinity of one non-isotropic line in the plane π. From Lemma 5, q corresponds to the point at infinity, at which the line on the plane π is perpendicular to

World Academy of Science, Engineering and Technology
International Journal of Mathematical and Computational Sciences
Vol:5, No:12, 2011

the line containing the point p at infinity,

$$(m_i m_j, pq) = -1.$$

Taking line eg as an example, we will discuss how to solve the vanishing point of a line which is orthogonal to one of diameter of virtual circle. Suppose v_5 is the vanishing point of line eg which is orthogonal to line at vanishing point v_6. v_6 can be gotten based on Lemma 4, Lemma 5 and cross-ratio invariance, and then the equation is as follows

$$v_6^T \omega v_5 = 0 . \qquad (15)$$

Combing with Equation (8) and (15), three constraint equations can be established about ω. Similarly, n constraint equations with the form of Equation (10) can be obtained from n diameters of a virtual circle

$$v_i^T \omega v_j = 0 ,$$

where v_i is a vanishing point of one diameter of a virtual circle, and v_j, v_i are two vanishing point on their mutually orthogonal directions. Let $\omega = \begin{bmatrix} \omega_1 & \omega_2 & \omega_3 \\ \omega_2 & \omega_4 & \omega_5 \\ \omega_3 & \omega_5 & \omega_6 \end{bmatrix}$, we have

$$\begin{cases} u_1 u_2 \omega_1 + (u_2 v_1 + u_1 v_2)\omega_2 + (u_1 + u_2)\omega_3 + v_1 v_2 \omega_4 + (v_1 + v_2)\omega_5 + \omega_6 = 0 \\ u_3 u_4 \omega_1 + (u_4 v_3 + u_3 v_4)\omega_2 + (u_3 + u_4)\omega_3 + v_3 v_4 \omega_4 + (v_3 + v_4)\omega_5 + \omega_6 = 0 \\ \vdots \\ \vdots \\ u_i u_j \omega_1 + (u_j v_i + u_i v_j)\omega_2 + (u_i + u_j)\omega_3 + v_i v_j \omega_4 + (v_i + v_j)\omega_5 + \omega_6 = 0 \end{cases} .$$

$$(16)$$

Let

$$f = \begin{bmatrix} \omega_1 & \omega_2 & \omega_3 & \omega_4 & \omega_5 \end{bmatrix}^T ,$$

$$A = \begin{cases} u_1 u_2 & u_2 v_1 + u_1 v_2 & u_1 + u_2 & v_1 v_2 & v_1 + v_2 & 1 \\ u_3 u_4 & u_4 v_3 + u_3 v_4 & u_3 + u_4 & v_3 v_4 & v_3 + v_4 & 1 \\ & & \vdots & & & \\ & & \vdots & & & \\ u_i u_j & u_j v_i + u_i v_j & u_i + u_j & v_i v_j & v_i + v_j & 1 \end{cases} ,$$

Equation (16) can be rewritten as $Af = 0$. When taking n images of the planar template under different views, the multiple constraint equations can be gotten about C, and f can be solved by the method of least squares to obtain ω. By Zhang's method [8], the intrinsic parameters can be calculated.

Outline of the algorithm is presented below:

Step 1. Print a square, stick it on the plane and at least take a picture.

Step 2. Obtain image coordinates of four vertexs of the square by Harris, and estimate homography matrix H.

Step 3. According to the Lemma 3, determine image intersection coordinates of virtual lines and a virtual circle, and image coordinates of circular points.

Step 4. Obtain vanishing points of parallel sides of the square

by solving image intersections of parallel sides.

Step 5. According to Lemma 4, obtain vanishing points of two diagonals of the square.

Step 6. According to Lemma 4 and Lemma 5, obtain any of virtual lines and its vanishing point of orthogonal lines.

Step 7. Obtain ω by the method of least squares, and then obtain K by Zhang's method [8].

IV. EXPERIMENTS

A. Experiments with Simulated Data

The values of camera intrinsic parameters are set to $f_u = 1000$, $f_v = 1100$, $u_0 = v_0 = 0$, $s = 0$ in simulation experiments. Simulations adopt three images which correspond to extrinsic parameters

$$R_1 = \begin{bmatrix} 0.8080 & 0.4106 & -0.4225 \\ 0.0695 & -0.7785 & -0.6238 \\ -0.5850 & 0.4747 & -0.6576 \end{bmatrix}, T_1 = \begin{bmatrix} -142.56 & -34.891 & 521.456 \end{bmatrix}';$$
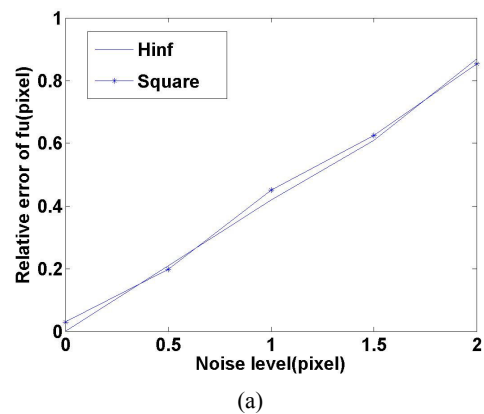
$$R_2 = \begin{bmatrix} -0.9993 & -0.0065 & 0.0361 \\ -0.0115 & -0.8780 & -0.4785 \\ 0.0348 & -0.4785 & 0.877 \end{bmatrix}, T_2 = \begin{bmatrix} -142.56 & -34.891 & 67.6 \end{bmatrix}';$$
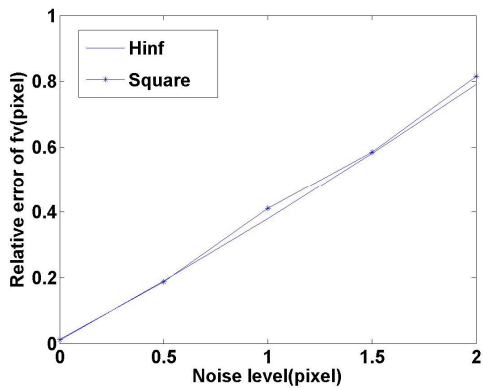
$$R_3 = \begin{bmatrix} -0.0002 & -0.9244 & -0.3815 \\ 0.0004 & -0.3815 & 0.9244 \\ -1.0000 & 0.0000 & 0.000 \end{bmatrix}, T_3 = \begin{bmatrix} -100 & 50 & 260 \end{bmatrix}',$$

respectively. The origin of WCS is the intersection of two diagonals of the square. We adopted three virtual lines, of which the corresponding slopes are $\frac{\pi}{12},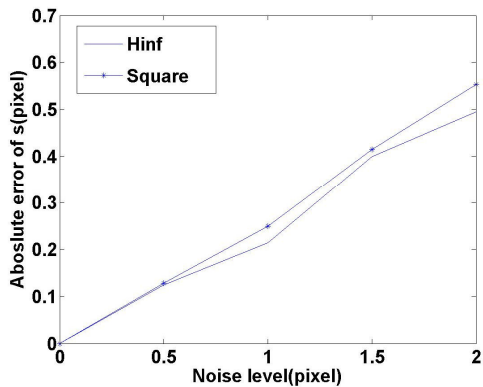 \frac{\pi}{6}, \frac{\pi}{3}$. In order to test the robustness of our proposed method, add the Gaussian noise where the mean value is zero and the mean square error is from 0.1 pixels to 5 pixels on the position of pixels. 200 independent experiments can be executed for each noise level, and solve their averages.

In the same camera parameters setting, carry out a comparative study between ours and Wang Guanghui's method [12] with skew factor $s=0$. The algorithm is denoted by Square in this paper, and Wang Guanghui's algorithm is denoted by Hinf. Comparisons of two algorithms are as follows (Fig. 4):

(a)

World Academy of Science, Engineering and Technology
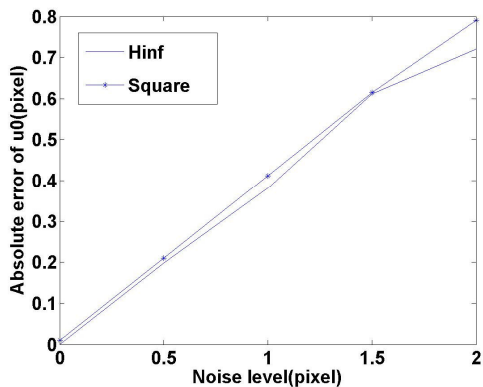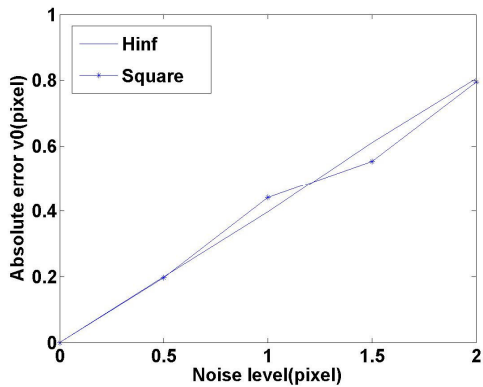International Journal of Mathematical and Computational Sciences
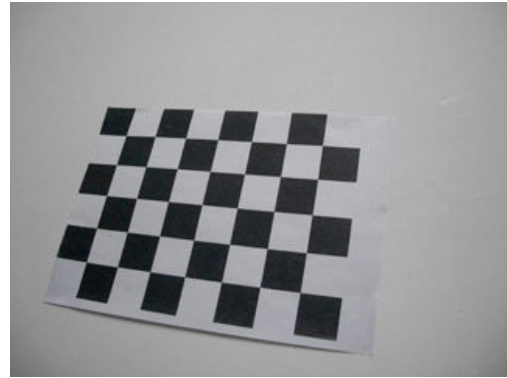Vol:5, No:12, 2011

(b)

(c)

(d)

(e)
Fig. 4 Accuracy of two methods concerning the noise level

B. Experiments with Real Images

The factual data can be used for comparing and testing two proposed algorithms. The kind of camera is a CCD digital camera where the size of the image is 320×240. Fig. 5 (a) and (b) are two photos from different calibration templates as follows.

(a) Calibration plane of Wang Guanghui
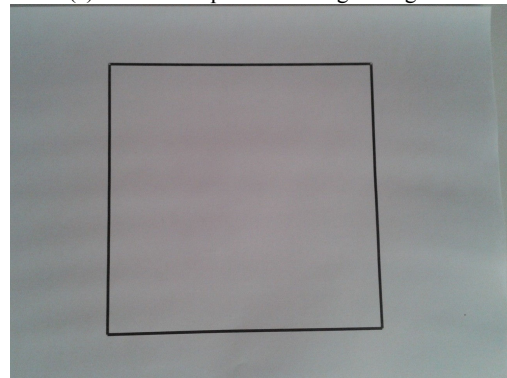
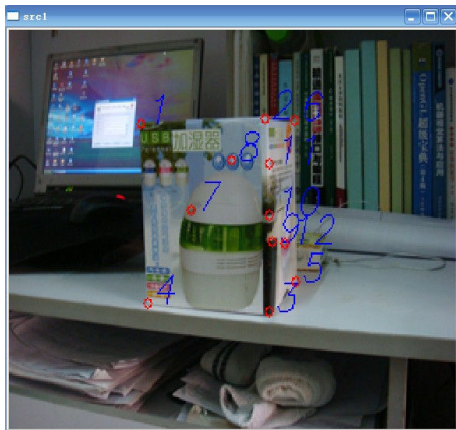(b) Calibration plane of this paper
Fig. 5 Images of different calibration templates

We carried out a comparative test with Wang Guanghui's calibration algorithm. The results are as follows (Table I):

TABLE I
A COMPARATIVE CALIBRATION RESULTS BY THE PROPOSED METHOD (HINF) AND WANG GUANGHUI'S METHOD (SQUARE)

Camera Intrinsic Parameters	Hinf	Square
f_u	51.389731	50.982492
f_v	51.389731	50.982492
s	51.389731	50.982492
u_0	51.389731	50.982492
v_0	51.389731	50.982492

In addition, we executed the 3D reconstruction by the calibration results as follows

World Academy of Science, Engineering and Technology
International Journal of Mathematical and Computational Sciences
Vol:5, No:12, 2011

(a) The first viewpoint

(b) The second viewpoint

Fig. 6 Images and matching points under different viewpoints
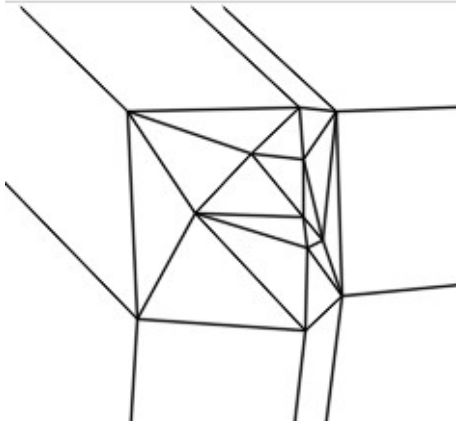

Fig. 7 Delaunay triangulations of characteristic points in the first viewpoint
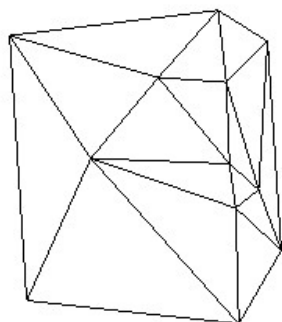

Fig. 8 Delaunay triangulations of the 3D points

(a)   (b)

(c)

Fig. 9 (a), (b) and (c) Results of 3D reconstruction under different viewpoints with texture mapping

V. CONCLUSIONS

In this paper, use a square as calibration template. In the square, two diagonals as the diameter, the intersection of two diagonals as the center of a circle creates a virtual circle, and the intersection of diagonals are used as the beam-center of beams of virtual lines. First, the homography matrix H is estimated from the four vertexs of the square to obtain image coordinates of the circular points and the intersections of the virtual circle and virtual lines. In additional, based on the cross-ratio invariance of projective transformation and conjugation between orthogonal vanishing points and circular points, the vanishing points of any of lines and the orthogonal vanishing points of them can be solved on the beam of virtual lines. So, IAC can be obtained by solving the constraint equations which are made up of mutually orthogonal vanishing points. Further, intrinsic parameters are determined through Zhang's decomposing method. Experimental data show that the algorithm is feasible and available, have a certain precision and robustness. In this paper, the homography matrix H is determined only by four vertices of a square, so the accuracy of four vertices affect the results of calibration. Therefore, in order to effectively improve the accuracy and the robustness of the algorithm, we can consider checkerboard as calibration plane.

World Academy of Science, Engineering and Technology
International Journal of Mathematical and Computational Sciences
Vol:5, No:12, 2011

REFERENCES

[1] Hartley R., "Estimation of relative camera positions for uncalibrated cameras", *In Proceedings of the European Conference on Computer Vision*, pp. 579-387, 1992.

[2] Maybank S.J., Faugeras O.D., "A theory of self-calibration of a moving camera", International Journal of Computer Vision, vol. 8, pp. 123-151, Feb. 1992.

[3] Hartley R., "Self-calibration of stationary cameras", *International Journal of Computer Vision,* vol. 22, pp. 5-23, Jan. 1997.

[4] Dron L., "Dynamic camera self-calibration of from controlled motion sequences", *In Proceedings of the IEEE Conference on Computer Vision and Pattern Recognition*, pp. 501-506, 1993.

[5] Du F., Brady M., "Self-Calibration of the intrinsic parameters of cameras for active vision systems", *In Proceedings of the IEEE Conference on Computer Vision and Pattern Recognition*, pp. 477-482, 1993.

[6] Pollefeys M., Koch R., Gool L.V., "Self-Calibration and metric reconstruction in spite of varying and unknown internal camera parameters", *In Proceedings of the International Conference on Computer Vision*, Bombay, pp. 90-95, 1998.

[7] Sturm P., "Critical motion sequences for monocular self-calibration and uncalibrated Euclidean reconstruction", In Proceedings of the IEEE Conference on Computer Vision and Pattern Recognition, 1100-1105(1997).

[8] Zhang Z., "A flexible new technique for camera calibration", *IEEE Transactions on Pattern Analysis and Machine Intelligence*, vol. 22, pp. 1330-1334, Nov. 2000.

[9] Meng X.Q., Li H., Hu Z.Y., "A new easy camera calibration technique based on circular points", *Journal of Software*, vol. 13, No. 5 pp. 957-965, May. 2002.

[10] Wu F.C.,Wang G.H.,Hu Z.Y., "A linear approach for determining intrinsic parameters and pose of cameras from rectangles". *Journal of software*, vol. 14, pp. 703-712, Feb. 2003.

[11] Xinju Li, Haijiang Zhu, Fuchao Wu, "Camera calibration based on coplanar similar geometrical entities". *PR&AI*. vol. 17, pp. 457-461, Apr. 2004.

[12] Guanghui Wang, Q.M. Jonathan Wu, Wei Zhang, "Kruppa equation based camera calibration from homography induced by remote plane", *Pattern Recognition Letters*, vol. 29, pp. 2137-2144, Aug. 2008.

[13] Hui Wang, Yue Zhao, "A new planar circle-based approach for camera self-calibration", *Journal of Computational Information Systems*, vol. 6, pp, 2877-2883, Sep. 2010.

[14] Yue Zhao, Hui Wang, "Conic and circular points based camera linear calibration", *Journal of Information & Computational Science*, vol. **7**, pp. 2478-2485, Dec. 2010.

[15] Yue Zhao, Hui Wang, Xiaofu Wang, "A Conic-Based Approach for Camera Linear Self-calibration", *Journal of Information & Computational Science*, vol. **7**, pp. 1959–1966, Sep. 2010.

[16] Hui Wang, Yue Zhao, Jianping Li, "Innovation experiment based on circular points and Laguerre theorem in computer vision", *In Proceedings of 2nd International Conference on Education Technology and Computer*, pp. 25-28, 2010.

[17] Harris C.G., Stephens M. J., "A combined corner and edge detector", *In Proceedings of Fourth Alvey Vision Conference*, pp. 147-151, 2001.

[18] Yunyoung Nam, Junghun Ryu, "Learning spatio-temporal topology of a multi-camera network by tracking multiple people", *Proceedings of World Academy of Science, Engineering And Technology*. vol. 24, pp. 175-180, Oct. 2007.

[19] Fuchao Wu, *Mathematical methods in computer vision*, Beijing: Science Press, 2008.

[20] Hartley R., Zisserman A., *Multiple view geometry in computer vision*, Cambridge: University Press, 2000.

Yue Zhao. He is a Senior Lecturer at the School of Mathematics and Statistics, University of Yunnan, China. His main research interests are in the areas of computer vision and computer graphics. He is particularly interested in the development and use of systems methodologies and tools to support managerial and learning activities in the above areas.

Chao Li. He received the B.S. and M.S. degree in School of Applied Mathematics from Taishan normal university, Shandong, Republic of China, in 2009. He is pursuing a doctorate in the School of Mathematics and Statistics at Yunnan University. His research interests include computer vision, applied mathematics and biomedical applications.